2022

Simultaneous measurement of temperature and strain in electronic packages using multi-frame super-resolution infrared thermography and digital image correlation

Sara K. Lyons

Justin Weibel
jaweibel@purdue.edu

Suresh V. Garimella

Lyons, Sara K.; Weibel, Justin; and Garimella, Suresh V., "Simultaneous measurement of temperature and strain in electronic packages using multi-frame super-resolution infrared thermography and digital image correlation" (2022). *CTRC Research Publications.* Paper 393.
http://dx.doi.org/10.1115/1.4054263

Simultaneous Measurement of Temperature and Strain in Electronic Packages using Multiframe Super-Resolution Infrared Thermography and Digital Image Correlation

Sara K. Lyons, Aditya Chandramohan, Justin A. Weibel,

and Suresh V. Garimella[1]

Cooling Technologies Research Center, School of Mechanical Engineering

Purdue University, West Lafayette, Indiana 47907 USA

Abstract

For microelectronic components and systems, reliability under thermomechanical stress is of critical importance. Experimental characterization of hotspots and temperature gradients, which can lead to deformation in the component, relies on accurate mapping of the surface temperature. One method of non-invasively acquiring this data is through infrared (IR) thermography. However, IR thermography is often limited by the typically low resolution of such cameras. Additionally, the unique surface finish preparations required to infer physical deformation using digital image correlation (DIC) generally interferes with the ability to measure the temperature with IR thermography, which prefers a uniform high emissivity. This work introduces a one-shot technique for the simultaneous measurement of surface temperature and deformation using multiframe super-resolution-enhanced IR imaging combined with digital image correlation (DIC) analysis.

[1] Currently President, University of Vermont

Multiframe super-resolution processing uses several sub-pixel shifted images, interpolating the image set to extract additional information and create a single higher-resolution image. Measurement of physical deformation is incorporated using a test sample with a black background and low-emissivity speckle features, heated in a manner that induces a non-uniform temperature field and stretched to induce physical deformation. Through processing and filtering, data from the black surface regions used for surface temperature mapping are separated from the speckle features used to track deformation with DIC. This method allows DIC to be performed on the IR images, yielding a deformation field consistent with the applied tensioning. While both the low- and super-resolution data sets can be successfully processed with DIC, super-resolution helps reduce noise in the extracted deformation fields. As for temperature measurement, using super-resolution is shown to allow for better removal of the speckle features and reduce noise, as quantified by a lower mean deviation from the spatial moving average.

Introduction

Hotspots are a serious concern in electronics packaging, both for the thermal and mechanical stresses they cause [1]. These stresses can cause damage to the system, and pose reliability risks as power and performance demands increase. Standard techniques to measure temperature and deformation separately are in existence, but the one-shot measurement approach developed here using a model system can be applied across various industrial applications to reduce costs, simplify the experimental testing required, and streamline qualification procedures for thermomechanical characterization of electronics packages and other components.

There are many standard methods to measure temperature, ranging from local spot measurements to surface mapping techniques. Thermocouples [2], thermoelectric probes [3], and

thermochromic liquid crystals [4] all require discrete sensors to be applied to the target surface. Microcantilevers can also be used as discrete sensors embedded in a medium to capture near-field data [5]. Other measurement techniques include infrared thermography [6,7], fluorescence-based thermography [8], and thermoreflectance thermography [9]. Among these methods, infrared thermography is especially attractive for electronics packaging systems as it allows for non-contact surface measurements across an entire field of view. This method of surface temperature measurement is typically conducted on a sample with a uniform emissivity, which can be achieved with an applied high-emissivity coating if necessary. This technique can be applied to non-uniform emissivity surfaces with emissivity mapping [6,10].

Digital image correlation (DIC), a method to measure the deformation of a surface [11], is non-invasive and can provide information over an entire region of interest. Traditionally, digital image correlation is conducted with a visual camera and requires a high-contrast pattern on the surface. Images of the surface are compared before and after deformation, and matching the location of pattern elements between the images enables the calculation of deformation and strain in the material. As a mature technique, there are known desirable surface patterns for the coatings, multiple options for post-processing, and best practices for determining processing parameters. Digital image correlation typically relies on surfaces with high contrast patterns with unique, trackable features, which stands in direct contrast to the uniform surface characteristics preferred in conducting infrared thermography temperature measurements [12]. Past efforts to combine these techniques for the simultaneous measurement of both temperature and deformation have tried to overcome these contradictory needs.

Simultaneous temperature and deformation measurements have been demonstrated through a combination of infrared thermography and digital image correlation. Wang et al. [13]

developed a process to simultaneously measure temperature and deformation in a thin aluminum sample by preparing one side for infrared thermography and the other side for digital image correlation with a visual camera. Post-processing was used to align the data sets from the two sides of the sample. Maynadier et al. [14] presented simultaneous temperature and deformation measurements on a shape memory alloy sample. While deformation measurements were calculated from the infrared data collected from one side of the sample, access to the other side was still required in a separate calibration step. While these studies provide examples of combined infrared thermography and digital image correlation techniques, imaging of only a single surface with an infrared camera to extract both temperature and deformation measurements is currently an area of further interest.

Simultaneous infrared thermography and digital image correlation on a surface with a single infrared camera is possible, as shown by Wang et al. [15] to track the deformation of a sample during a tensile test. In general, this combined approach is challenged by the lower pixel number/resolution of most infrared camera sensors [16] compared to that of visual cameras typically employed for standalone DIC. As in all imaging applications, a lens configuration that captures a larger surface region of interest also has a necessary tradeoff in image resolution. The tradeoff between sensor limitations and field of view can be overcome by enhancing image resolution through the use of multiframe super-resolution processing. Multiframe super-resolution is a technique by which a high-resolution image can be generated from a collection of low-resolution images. The images must be acquired with a subpixel displacement from each other, generating a set of images of the same subject but with more information than a single image at the native pixel resolution. These images are then interpolated together with weighted averaging, generating the high-resolution image. While this is a well-developed technique for visual imaging

[17], our recent work demonstrated that super-resolution processing techniques can also be successfully applied to infrared imaging with robust error quantification [10]. This is a promising development that is leveraged in the current study to help enable simultaneous DIC with improved-resolution IR image data.

This study investigates the benefits of super-resolution while exploring a novel single-surface, one-shot infrared thermography and digital image correlation method to improve the acquisition of material deformation and surface temperature information. The method prepares a single surface in a manner that serves the needs of both IR imaging and DIC, and with appropriate processing of the images captured, it overcomes the need for a uniform emissivity surface. The preparation of the surface and the facility used for demonstration of the technique, along with the experimental procedures, are first introduced. Image processing to create a super-resolution image, as well as the separation of the high-emissivity data for thermal measurements from the markers for DIC, are then discussed. The results of this work show that a combined single-surface, one-shot approach to infrared thermography and digital image correlation, in conjunction with super-resolution image processing, is possible without sacrificing the usability of the temperature data captured or the ability to calculate the extent of surface deformation.

Experimental Methods

For this single-surface, one-shot technique, the requirements of both IR imaging and DIC processing had to be incorporated into the test surface. The experimental setup also had to incorporate a method to capture sub-pixel shifted images for super-resolution processing. These requirements were addressed by creating a sample with a dark, high-emissivity background coating along with a coating of contrasting low-emissivity speckles that could be distinguished in IR

images. These coatings need to be flexible enough to stretch without cracking to create the deformation needed for DIC. The experimental facility was designed with the capability to tension the sample by a controlled amount and generate the necessary shifted states for super-resolution processing. The creation of the dual-purpose surface and experimental facility are detailed further below.

Test Sample

The sample used for technique demonstration was a stretchable sheet of latex rubber. The top face of the sample was sprayed with a black coating (Rust-oleum® LeakSeal®) to create a high emissivity background, following the manufacturer's coating instructions to create a uniform base layer. Speckles were applied on the cured background by spraying gold paint (Krylon Metallic Paints Gold 1706) at a controlled distance from the surface. The gold paint, of lower emissivity than the background coating, was chosen so that the speckles could be distinguished from the background in the infrared images. While the data recorded from these speckle features will not provide accurate temperature data, those features in the infrared images are instead isolated for use as markers for the digital image correlation process. The black matte finish of the background coating is expected to have an emissivity >0.95, similar to traditional black paints, while the metallic paint has a notably lower emissivity due to the finish, as is evident from viewing the surface with the IR camera when at a uniform temperature. A visual image of an illustrative region of the test sample can be seen in the inset of Figure 1.

Experimental Facility

The test facility, intended as a model system to demonstrate the approach, depicted in Figure 1, was designed to incorporate the ability to separately apply a desired heating condition and deform the sample *in situ*, and to generate the sub-pixel shifts required for super-resolution imaging with the infrared camera. A simple mode of deformation was chosen to ensure repeatable and verifiable test conditions. The sample is held horizontally with the patterned side oriented up, secured at each end over tensioning cylinders. The cylinders can be rotated to adjust the strain in the sample without causing significant out-of-plane displacements, and then locked into place while images were taken. The infrared camera (FLIR SC7650), fitted with a 25 mm lens and 6.35 mm long spacer tube, was mounted above the sample and oriented to be perpendicular to the sample surface. This configuration produced images with an original pixel resolution of 144.3 µm.

Hotspot heating was induced using a 0.125 in (3.175 mm) cylindrical cartridge heater. The heater was placed under the sample and held vertically in place with insulating foam, with the tip slightly separated from the latex sample to ensure it would not contact the sample as it was stretched. The temperature of the heater, as measured using a thermocouple attached to the top of the cartridge, was controlled with a feedback system (Temp-o-Trol TOT-1200). This heater temperature was set to 90 ºC to induce a centrally heated area on the surface creating a non-uniform temperature field. The surface was shielded from external convective currents and other environmental disturbances using an enclosure as shown in the figure. The sample was mounted on two orthogonal differential micrometer stages, with a spatial resolution of 0.5 µm each, allowing for motion in the in-plane x- and y-directions. This enabled the sub-pixel shifting, in both directions, as necessary for the super-resolution image processing.

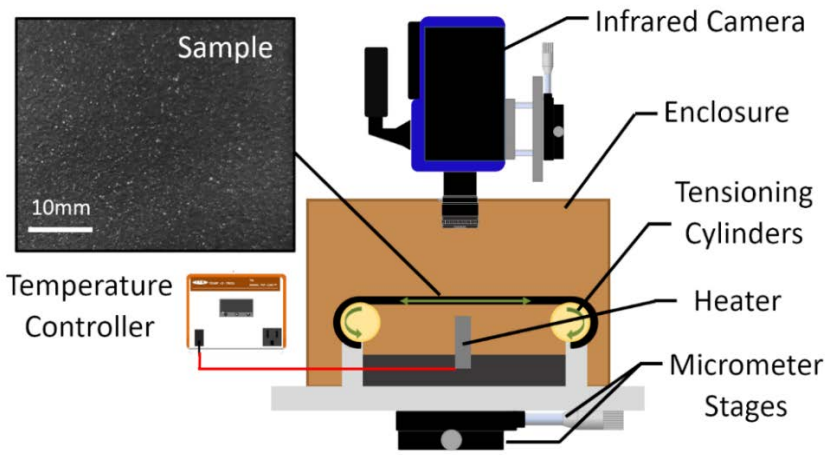

Figure 1. Schematic diagram of experimental facility with an inset image of the speckled test surface.

Experimental Procedure and Calibration

At the start of the experiment, the sample was mounted on the cylinders and secured in place. The cylinders were then rotated in opposing directions so that the sample was taut, and then locked into place. The heating element was turned on and the resulting hot spot in the image field allowed to reach steady-state thermal conditions. Holding these conditions steady, a complete set of images was obtained to generate the super-resolution image. In this work, the target resolution was chosen to be five times the original camera resolution. To achieve this, a square grid of 25 sub-pixel shifted images was captured for each tension state, with a shift of 25 μm between each image. Each image set started with capturing the corner frame, followed by acquisition of the remaining shifted images row-by-row. This was repeated to produce the 5×5 grid of component images.

The sample was measured in three tension states, namely the initial taut state and then two successively more tensioned (stretched) states. Each additional tension state is achieved by rotating the cylinder at each end outward by 15 deg. The complete set of images is taken in the same order

as described above, starting from the same stage position, for each measurement taken. The results presented here are for the deformation of the sample from the second to the third state.

A black body calibration was conducted alongside the experiments. This calibration was conducted using a differential blackbody calibrator (SBIR DB-04) over a range of temperatures covering the expected experimental range. The camera settings for the calibration matched those used for the experiments – a frequency of 100 Hz and an integration time of 750 μs.

Processing Methods

Overview

After obtaining all images at each tension state, the data are processed to generate the collection of low-resolution images and the associated super-resolution image data from the tests. In order to assess the effects of super-resolution on both the deformation and thermal results, a single low-resolution image and the final super-resolution image are further processed using the same steps to prepare the input images for digital image correlation and to recover the corrected temperature field (i.e., with the inaccurate speckle data removed). An overview of the processing procedure is shown in Figure *2*, and each step is detailed further in the following subsections.

The overall objective of the processing is to isolate the speckles which are used to conduct DIC, from the background data which can be used to extract the surface temperature. Therefore, the first several steps of the process aim to create a binary image of the speckles only. The binary image of the speckles is first obtained through two phases of filtering applied to the original infrared data. First, a threshold is applied to the original temperature map to generate a normalized greyscale image from the IR data. This greyscale image is then further reduced to a binary map, with additional filters applied to reduce noise. The resulting binary speckle map for each case can

then be used as an input for DIC processing to yield a displacement map. Separately, the same binary speckle map is used to mask out the low-emissivity regions of the IR data, leaving only the corrected temperature data from the black background.

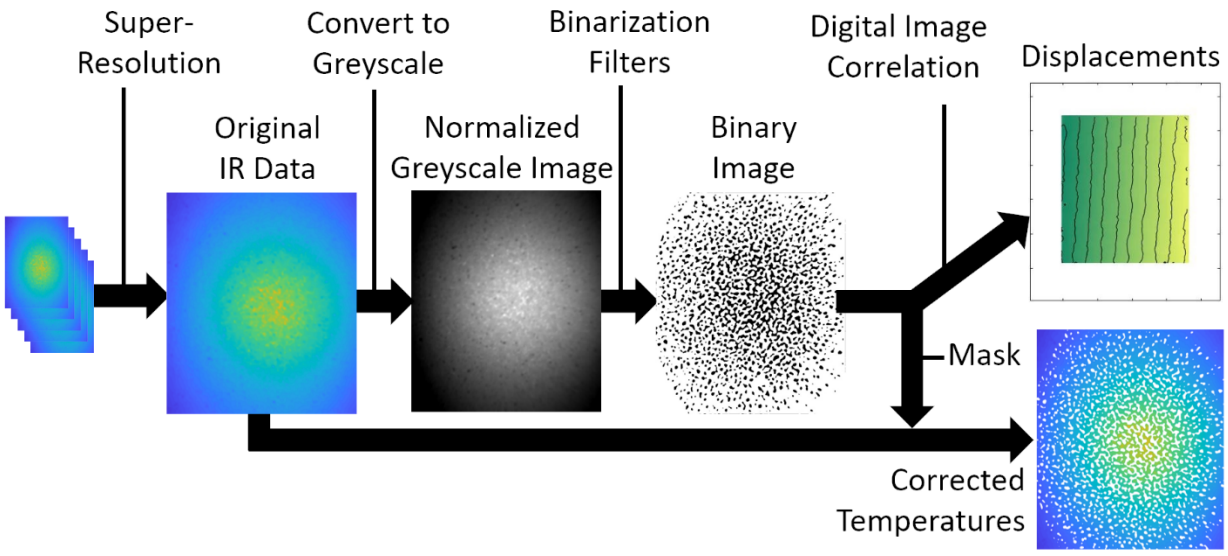

Figure 2. Image processing map, starting from the collected images and resulting in a displacement map and a temperature map.

Preparation of the Binary Image

At each tension state, the super-resolution image was generated from the collection of low-resolution images following the same procedures as described in detail in our previous work [10]. Briefly, the data from the original images were first mapped into an *x*-*y* plot using the known displacements, and then interpolated into the super-resolution grid using a natural neighbor approach. A Gaussian noise filter is then applied as the final step of the super-resolution image generation. As a benchmark comparison for the enhanced displacement and temperature mapping performance of the super-resolution images, a single frame from each tension state is used as a low-resolution image to be processed and compared with the super-resolution results.

After super-resolution enhancement, to create the binary image used as an input for DIC and to mask out low-emissivity points from the temperature map, the full image was cropped to remove unusable data around the image edges. For example, areas over the cylinders that were outside the effects of the heater and therefore had low contrast were removed along with edge regions that appeared out of focus due to out-of-plane rotation of the material. The image was then converted to greyscale, using the minimum and maximum signal values in a high-contrast region of the image as threshold values for normalization. Filters were applied to the greyscale image to remove grid pattern artifacts that appear due to variations in the component images of the super-resolution processing. The greyscale image was filtered using a median and an averaging filter to address this linear noise. To increase the contrast, the filtered greyscale image was processed with a difference-of-Gaussian filter [18], and then binarized. The processing parameters used to obtain the speckle map were appropriately scaled to create equivalent processing conditions between the side-by-side low-resolution benchmark and super-resolution data sets. For example, the images were cropped to the same physical sizes and the greyscale thresholding region dimensions were kept consistent between the low-resolution benchmark and the super-resolution images. The super-resolution and image processing procedures were all conducted in MATLAB [19].

At the end of this image preparation process, a binary map of features on the sample surface for each tension state is created from the original infrared data. These binary maps are directly used for the DIC analysis to calculate the surface displacement. Additionally, these feature maps are used as masks to remove the speckle features from the original IR data to generate the temperature map of the surface. Because the speckle features are of a different emissivity than the background used for temperature calibration, the IR data in the speckles does not correspond to an

accurate surface temperature. Using the binary maps generated, the locations of the features in each image can be determined and removed from the IR dataset before showing the corrected temperature data corresponding to only the background (black-painted) areas.

Digital Image Correlation

The binary speckle maps were used as the inputs for digital image correlation analysis using Ncorr, an open-source MATLAB program [20]. The isolated binary speckle fields retrieved from the temperature maps were input along with an image of the desired margins to define the region of interest. For the super-resolution case, the maps were processed using a subset radius of 35 pixels and spacing of 5 pixels, to ensure that the subset radius was smaller than the margin around the region of interest, to avoid potential edge issues. These values were chosen to allow the same processing scheme to be applied to both the super-resolution and low-resolution images.

In conducting the DIC on the low-resolution image set, the subset radius and spacing are scaled by five, corresponding to the scaling of the resolution between the low- and super-resolution images, to create a processing case equivalent to the one used for the super-resolution case. That is, the processed region of interest and subset radius were set so that they would correspond to the same physical areas of the images across the low- and super-resolution cases. There was one exception to this consistent scaling, in particular regarding the subset radius. Strictly following the scaling would have required a 7-pixel subset radius for the low-resolution case; however, the smallest possible subset available in the processing software of 10 pixels was instead used. A comparison of the regions of interest and subset regions can be seen in Figure *3*. These show the equivalence in the processing regions between the two resolution levels. Additionally, from this image, the difference between the low- and super-resolution speckle maps is visible.

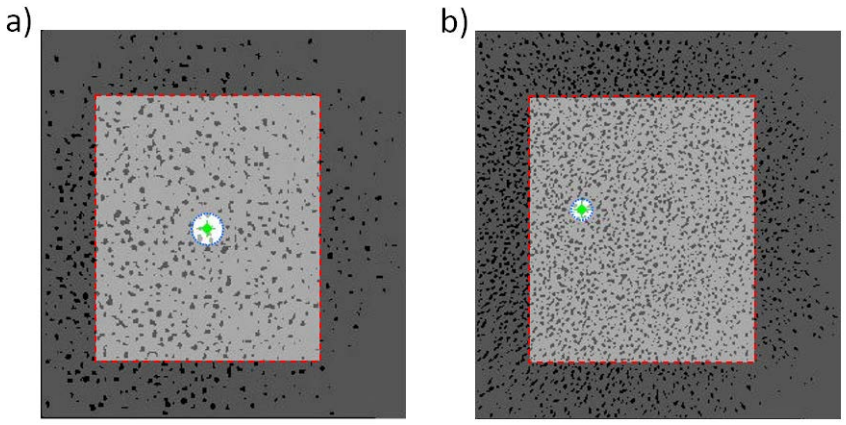

Figure 3. The digital image correlation processing subsets for the (a) low-resolution and (b) super-resolution cases where the interior of the red (dashed line) rectangular section is the region of interest, the interior of the blue (dotted line) circular region is the calculation subset, and the green point at the center of the circle is the starting seed location.

Results and Discussion

Digital Image Correlation Results

Since the sample deformation for this work was achieved by applying tension symmetrically from two ends, the results have no x-direction displacement along the longitudinal centerline and no y-direction (transverse) displacement along the horizontal centerline. The tensioning mechanism is expected to result in 3.33 mm of longitudinal displacement at the very edge of the sample, corresponding to one step of cylinder rotation between two tensioned states. Assuming continuous elastic tension, this translates to a displacement at the edge of the region of interest of 1.24 mm away from the centerline. The resulting longitudinal and transverse displacement fields from the digital image correlation processing on both the low-resolution and super-resolution binary speckle maps extracted from the IR data are shown in Figure 4. After conducting DIC on both the low- and super-resolution binary image sets, the maximum absolute longitudinal displacements from the centerline at each edge of the region of interest were

calculated to be 0.99 mm and 1.29 mm for the low-resolution set and 0.90 mm and 1.20 mm for the super-resolution set, close to the estimated displacements.

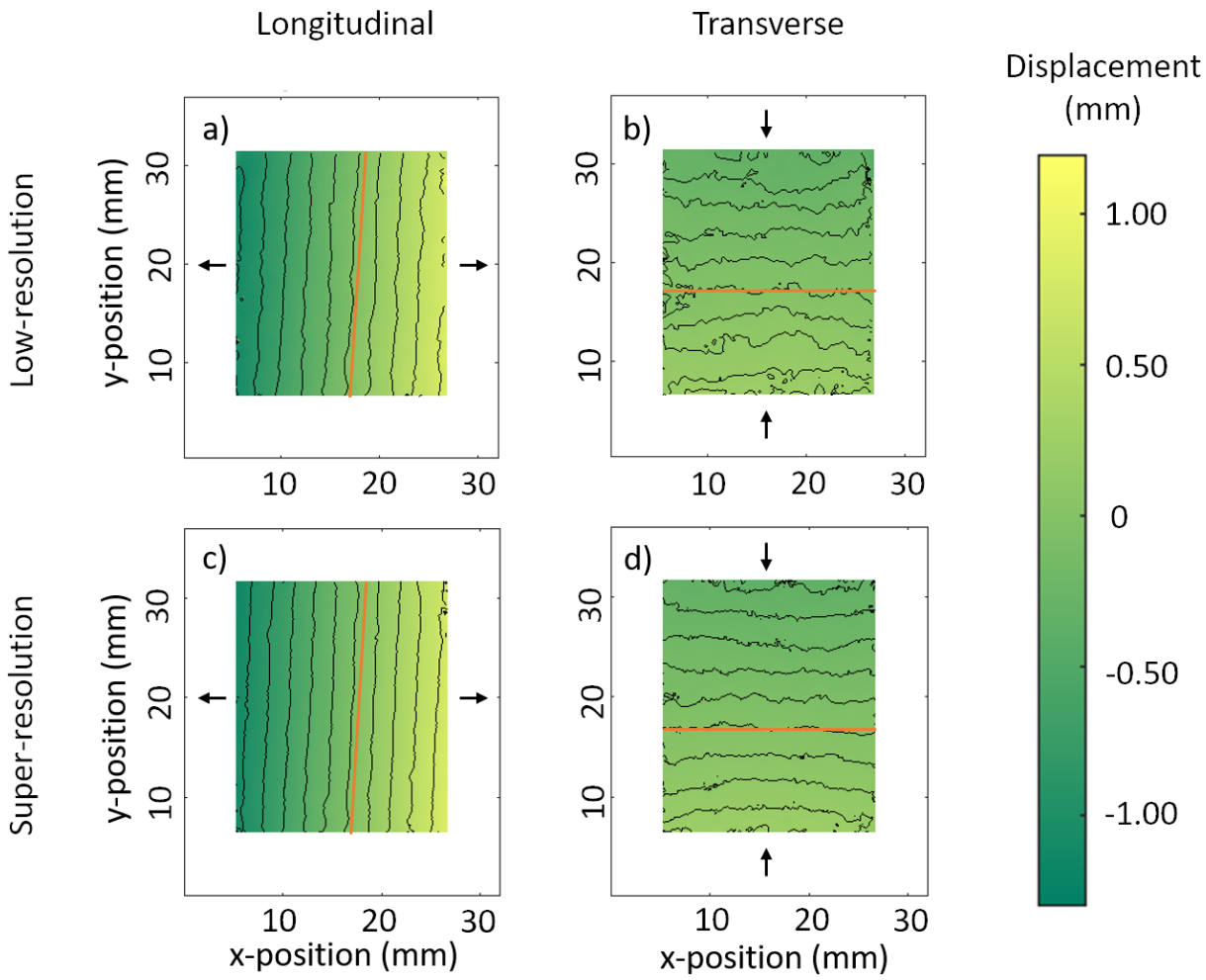

Figure 4. Contour fields of the longitudinal (left) and transverse (right) displacement calculated using digital image correlation for the (a, b) low-resolution and (c, d) super-resolution cases.

An ideal map of longitudinal displacement would have a linear gradient with vertical contour isolines, and the transverse deformation would have curved contours that are symmetric about the transverse centerline. The contour maps from DIC processing reveal similar displacement results for the low- and super-resolution cases, also matching the expected contour

shapes. The contour maps show the elongation in the longitudinal direction, as regions to the left of the centerline experience a negative displacement and regions to the right experience a positive displacement (both away from the centerline). The contraction in the transverse direction can be seen as points above the centerline experience a negative displacement and points below the centerline experience a positive displacement (both towards the centerline). In both the transverse and longitudinal displacement maps, the super-resolution contours are smoother than at the low resolution. Additionally, the super-resolution case shows fewer edge artifacts in the displacement contours calculation. It is expected that when deformation fields have finer and more complex features, the increased resolution will offer a large benefit in terms of measurement accuracy.

The enhanced measurement performance of the super-resolution images is attributed to the smaller processing subsets in digital image correlation. The subset must be larger in low-resolution images relative to the image size in order to perform the digital image correlation. In addition to this processing resolution advantage, the smaller subset also means that more of the original field of view can be processed. Generally, when conducting DIC, the interrogated region should have a margin of at least one subset radius from the edge of the image. With the use of a smaller subset during super-resolution processing, this margin can be smaller and therefore more of the image is usable.

Temperature Mapping Results

In addition to creating the inputs for digital image correlation, the binary speckle maps are used as masks of the original IR data, as described in the Image Preparation section above. Figure *5* shows the original IR data and the corrected temperature fields (i.e., before and after removal of the speckle regions) for both the low- and super-resolution cases. The low-resolution corrected

temperature map shows that the speckles overall appear larger and have more open space between them compared to the super-resolution map; in the latter, it is possible to more precisely and selectively remove the speckles.

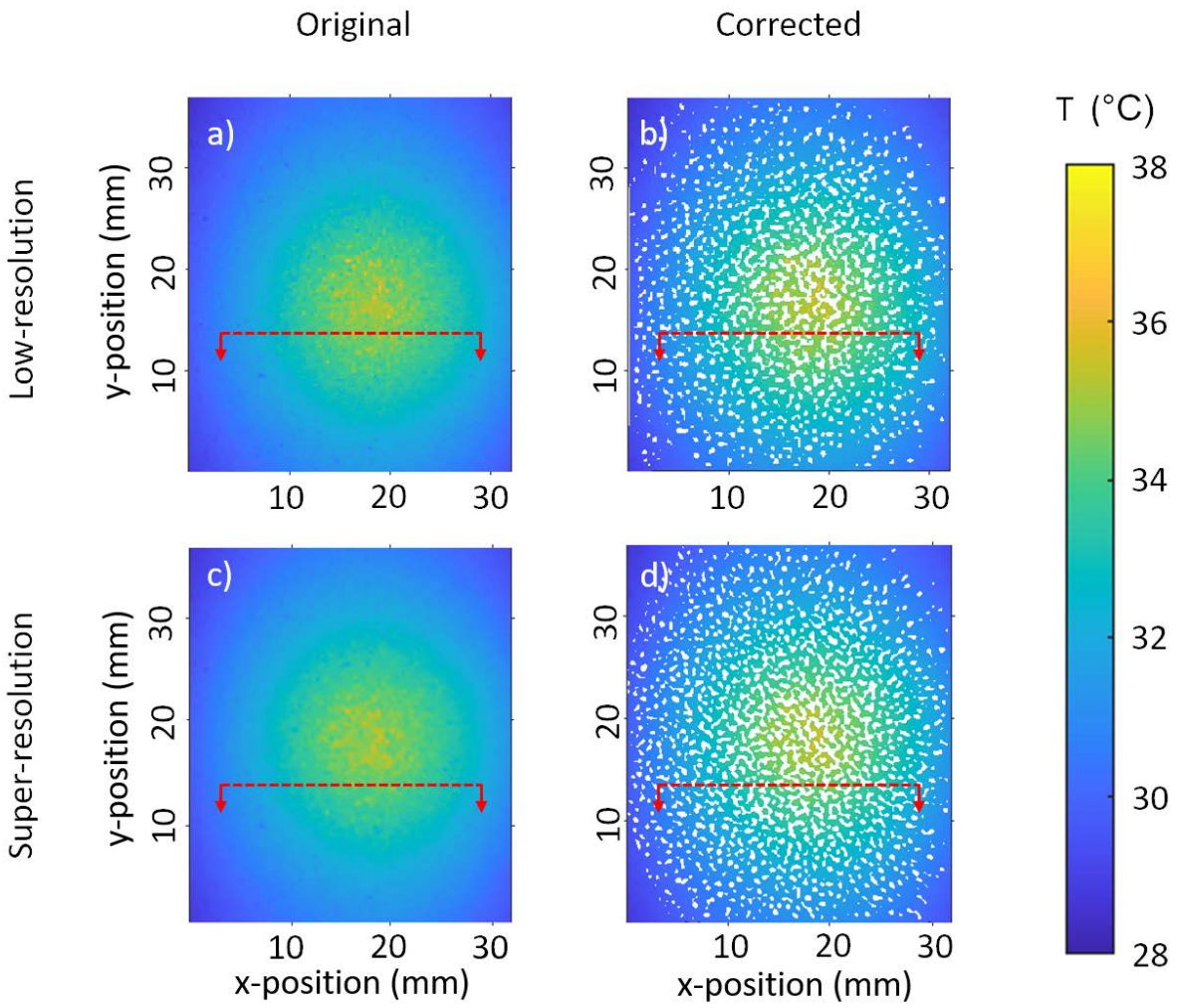

Figure 5. Temperature fields with and without speckles for (a, b) the low-resolution case and (c, d) the super-resolution case.

To more quantitatively characterize and compare the temperature results before and after removal of the speckle features, Figure 6 plots a rake of the temperature data across the width of the image (vertically offset from the center of the hotspot, with the rake location indicated in Figure 5). Also plotted is a moving mean across the rake of the original low- and super-resolution data

taken from the case before the speckles are removed. The window size for the moving mean covers ~16% of the width of the image. This curve is then used as a reference to evaluate outliers in the temperature data due to the presence of the speckles (before and after removal).

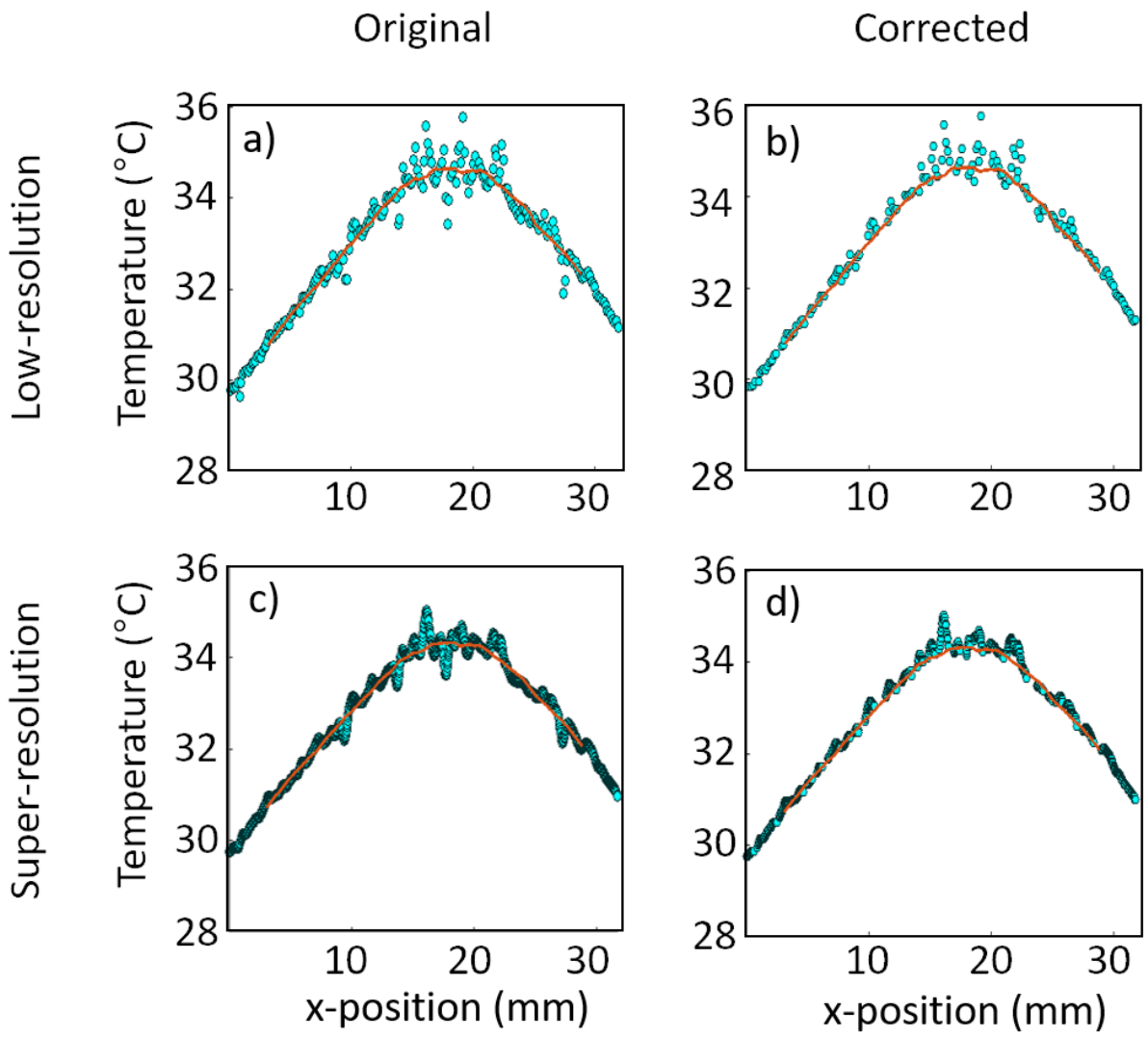

Figure 6. Temperature data along a horizontal temperature rake before and after the speckles are removed for (a, b) the low-resolution case and the (c, d) the super-resolution case.

The original IR data before the speckles are removed show significant fluctuation (observed as deviations from the moving average) that is attributed to the low-emissivity speckles which are not considered in the temperature calibration. The corrected temperature plots with the

speckles removed show the improvement achieved especially in the super-resolution case. The mean absolute deviation of the data from the local moving average reference is calculated for the cases with and without speckles, in low- and super-resolution. At both resolutions, this mean absolute deviation decreases with the speckles removed. In the low-resolution case, removing the speckles reduced the mean absolute deviation from 0.200 °C to 0.185 °C, while in the super-resolution case it reduces from 0.139 °C to 0.135 °C. These mean absolute deviations also clearly indicate that the use of super-resolution reduces the deviation both before and after the speckles are removed. The addition of super-resolution processing not only enables cleaner displacement fields through digital image correlation, but also more effective removal of DIC markers from thermal maps, thereby providing a benefit to this one-shot measurement of both quantities.

Conclusions

A new approach to simultaneous infrared thermography and digital image correlation introduces multiframe super-resolution image processing to yield a practical, one-shot approach. In this approach, a single infrared camera is able to capture the temperature and deformation at a surface, without any changes to the camera hardware or optics. The addition of super-resolution processing allowed for improved delineation of the speckle features when compared to the low-resolution case. The improved removal of these features is quantified as a decrease in the mean absolute deviation from a background reference, from 0.2 °C in the low-resolution raw IR data to 0.135 °C in the super-resolution temperature field. Additionally, the displacement maps from the digital image correlation processing were smoother and included fewer edge artifacts with the super-resolution input data. By improving on the native resolution of the infrared camera via multiframe super-resolution processing, a single-camera, single-surface approach to combined

infrared thermography and digital image correlation becomes a viable option for combined thermal and mechanical stress analysis.

References

[1] S. V Garimella, A. S. Fleisher, J. Y. Murthy, A. Keshavarzi, R. Prasher, C. Patel, S. H. Bhavnani, *et al.*, "Thermal challenges in next-generation electronic systems," *Trans. Components Packag. Technol.*, vol. 31, no. 4, pp. 801–815, 2008.

[2] L. Shi and A. Majumdar, "Recent developments in micro and nanoscale thermometry," *Microscale Thermophys. Eng.*, vol. 5, no. 4, pp. 251–265, 2001.

[3] H. H. Roh, J. S. Lee, D. L. Kim, J. Park, K. Kim, O. Kwon, S. H. Park, Y. K. Choi, and A. Majumdar, "Novel nanoscale thermal property imaging technique: The 2ω method. I. Principle and the 2ω signal measurement," *J. Vac. Sci. Technol. B Microelectron. Nanom. Struct.*, vol. 24, no. 5, pp. 2398–2404, 2006.

[4] M. Parsley, "The use of thermochromic liquid crystals in research applications, thermal mapping and non-destructive testing," in *Seventh IEEE SEMI-THERM Symposium*, 2002, pp. 53–58.

[5] S. Kim, K. C. Kim, and K. D. Kihm, "Near-field thermometry sensor based on the thermal resonance of a microcantilever in aqueous medium," *Sensors*, pp. 3156–3165, 2007.

[6] M. Vellvehi, X. Perpiñà, G. L. Lauro, F. Perillo, and X. Jordà, "Irradiance-based emissivity correction in infrared thermography for electronic applications," *Rev. Sci. Instrum.*, vol. 82, no. 11, 2011.

[7] A. Trigg, "Applications of infrared microscopy to IC and MEMS packaging," *IEEE Trans. Electron. Packag. Manuf.*, vol. 26, no. 3, pp. 232–238, 2003.

[8] D. L. Barton and P. Tangyunyong, “Fluorescent microthermal imaging - Theory and methodology for achieving high thermal resolution images,” *Microelectron. Eng.*, vol. 31, pp. 271–279, 1996.

[9] M. G. Burzo, P. L. Komarov, and P. E. Raad, “Noncontact transient temperature mapping of active electronic devices using the thermoreflectance method,” *IEEE Trans. Components Packag. Technol.*, vol. 28, no. 4, pp. 637–643, 2005.

[10] A. Chandramohan, S. K. Lyons, J. A. Weibel, and S. V. Garimella, “Error Reduction in Infrared Thermography by Multiframe Super-Resolution,” *J. Electron. Packag.*, vol. 140, no. 4, p. 041008, 2018.

[11] N. McCormick and J. Lord, “Digital image correlation,” *Mater. Today*, vol. 13, no. 12, pp. 52–54, 2010.

[12] M. Bornert, F. Hild, J.-J. Orteu, and S. Roux, “Digital image correlation,” in *Full-Field Measurements and Identification in Solid Mechanics*, Hoboken, NJ: ISTE Ltd./John Wiley and Sons Inc., 2013, pp. 157–190.

[13] X. Wang, J. F. Witz, A. El Bartali, and C. Jiang, “Infrared thermography coupled with digital image correlation in studying plastic deformation on the mesoscale level,” *Opt. Lasers Eng.*, vol. 86, pp. 264–274, 2016.

[14] A. Maynadier, M. Poncelet, K. Lavernhe-Taillard, and S. Roux, “One-shot Measurement of Thermal and Kinematic Fields: InfraRed Image Correlation (IRIC),” *Exp. Mech.*, vol. 52, no. 3, pp. 241–255, 2012.

[15] X. G. Wang, C. H. Liu, and C. Jiang, “Simultaneous assessment of Lagrangian strain and temperature fields by improved IR-DIC strategy,” *Opt. Lasers Eng.*, vol. 94, pp. 17–26, 2017.

[16] M. S. Alam, J. G. Bognar, R. C. Hardie, and B. J. Yasuda, “Infrared image registration and high-resolution reconstruction using multiple translationally shifted aliased video frames,” *IEEE Trans. Instrum. Meas.*, vol. 49, no. 5, pp. 915–923, 2000.

[17] M. G. Park, S.C., Park, M.K., Kang, “Super-Resolution Image Reconstruction: A Technical Overview,” *IEEE Signal Process. Mag.*, vol. 20, no. 3, pp. 21–36, 2003.

[18] D. G. Lowe, “Distinctive image features from scale-invariant keypoints,” *Int. J. Comput. Vis.*, vol. 60, no. 2, pp. 91–110, 2004.

[19] C. Mathworks, “MATLAB Primer.” The MathWorks, Inc, Natick, MA, 2018.

[20] J. Blaber and A. Antoniou, “Ncorr Instruction Manual.” 2017.